The ^{8}Be excess and search for the $X \to e^+e^-$ decay of a new light boson with NA64 detector

The NA64 Collaboration

April 2, 2017

Abstract

The $X \to e^+e^-$ decay of a new short-lived neutral boson, X, with a mass $m_X = 16.7$ MeV and coupling to electrons in the range $10^{-4} \lesssim \epsilon_e \lesssim 10^{-3}$ could explain the excess of e^+e^- pairs recently observed in the excited ^{8}Be* nucleus decays. If such X's exist, they could be searched for in a light-shining-through-a-wall experiment with a high energy electron beam. The electron energy absorption in a calorimeter (WCAL) is accompanied by the emission of bremsstrahlung X's in the reaction $eZ \to eZX$ of electrons scattering off a nuclei due to the $e-X$ coupling. A part of the primary beam energy is deposited in the WCAL, while the rest of the energy is transmitted by the X through the "WCAL wall" and deposited in another downstream calorimeter, ECAL, by the e^+e^- pair from the $X \to e^+e^-$ decay in flight. Thus, the X's could be observed by looking for an excess of events with the two-shower signature generated by a single high energy electron in the WCAL and ECAL.

In October 2016 NA64 took a short run to study feasibility of the search for the $X \to e^+e^-$ decay at H4 beamline with this method. A proposal based on the results of this run to perform an experiment aiming to probe the region of coupling strength $10^{-4} \lesssim \epsilon_e \lesssim 10^{-3}$ and mass $m_X = 16.7$ MeV by using 100-150 GeV electron beams from the H4 line is presented. The experiment can test for the first time the X parameter space with the sensitivity allowing either to exclude or observe the X boson in the run 2017 with the NA64 detector.

CERN-SPSC-2017-016 / SPSC-SR-211
02/04/2017

Executive summary

We propose new measurements dedicated to the sensitive search for the $X \to e^+e^-$ decay of a new short-lived neutral boson, X, with a mass 16.7 MeV and coupling to electrons in the range $2 \times 10^{-4} < \epsilon_e < 1.4 \times 10^{-3}$ which could explain an excess of e^+e^- pairs observed in the excited ^{8}Be* nucleus transitions.

If such X's exist, they could be searched for in a light-shining-through-a-wall experiment with a high energy electron beam. The electron energy absorption in a calorimeter (WCAL) is accompanied by the emission of bremsstrahlung X's in the reaction $eZ \to eZX$ of electrons scattering off a nuclei due to the $e - X$ coupling. A part of the primary beam energy is deposited in the WCAL, while the rest of the energy is transmitted by the X through the "WCAL wall" and deposited in another downstream calorimeter, ECAL, by the e^+e^- pair from the $X \to e^+e^-$ decay in flight. Thus, the X's could be observed by looking for an excess of events with the two-shower signature generated by a single high energy electron in the WCAL and ECAL. A proposal to perform such an experiment to probe the still unexplored area of coupling strength $10^{-4} \lesssim \epsilon_e \lesssim 10^{-3}$ and mass $m_X = 16.7$ MeV by using 100-150 GeV electron beams from the CERN SPS is presented. The search can provide for the first time coverage of the parameter space, which is intended to be probed by other searches, and either to exclude or observe the X boson in the run 2017 with the NA64 experiment.

The experiment could exploit the H4 beam-line at the CERN SPS, which can provide electrons with an energy up to $\gtrsim 150$ GeV. The detector consists of a compact, specially designed scintillator-tungsten electromagnetic (e-m) calorimeter of high longitudinal hermeticity, and additionally protected against the energy leak by high efficiency veto counters. It is also equipped with the tracker, beam defining scintillator counters, HCAL, and synchrotron radiation detectors which provide information for a high-purity tagging of the incoming electrons.

The feasibility study of the proposed search performed in a short run in October 2016 combined with extensive simulations show that with accumulated $n_{eot} \simeq 10^{11}$ electrons on target (eot) the projected sensitivity for the search of the $X \to e^+e^-$ decay mode is high enough to observe X if its coupling is lying in the range $2 \times 10^{-4} \lesssim \epsilon_e < 10^{-3}$. In case of non-observation the search will exclude a significant fraction of the X parameter space.

The experiment could be performed in two phases. In phase I in 2017, the goal is to optimize the detector components, to perform the search and measure the dominant backgrounds from the punch-through photons and hadrons (and possibly muons) contaminating the electron beam. In case of non-observation the goal for phase II in 2018 would be to run experiment in another detector configuration and at higher energy $\simeq 150$ GeV in order to reach the maximal sensitivity for the coupling strength in the region $10^{-3} < \epsilon_e < 2 \times 10^{-3}$ and fully exploit the potential of the detector after a possible upgrade, which might be necessary given the results of phase I. To reach this goal, accumulating a few 10^{10} eot at 150 GeV is mandatory. If an excess consistent with the signal hypothesis is observed, this would unambiguously indicate the presence of new physics.

1 Motivation

The experiment of Krasznahorkay et al. [1] in ATOMKI has reported observation of a 6.8 σ excess of events in the invariant mass distributions of e^+e^- pairs produced in the $^8Be^*$ excited state nuclear transitions to its ground state accompanied by an emission of an e^+e^- via internal pair creation. Feng et al. show that this anomaly can be interpreted as an emission of a new protophobic gauge boson followed by its prompt $X \to e^+e^-$ decay [2, 3] and provide a particle physics explanation of the anomaly consistent with all existing constraints assuming its coupling to electrons is in the range $2 \times 10^{-4} < \epsilon_e < 1.4 \times 10^{-3}$ and mass $M_X = 16.7$ MeV. Their models predict relatively large charged lepton couplings $\epsilon_e \simeq 0.001$ that can also resolve the discrepancy in the muon anomalous magnetic moment. They also contain vectorlike leptons at the weak scale that can be accessible to the near future LHC searches.

All this makes the search for such $X \to e^+e^-$ decay mode quite interesting and exciting. Below we show that NA64 is able to cover a significant region of the predicted parameter space, see Fig.1 from Ref.[2, 3].

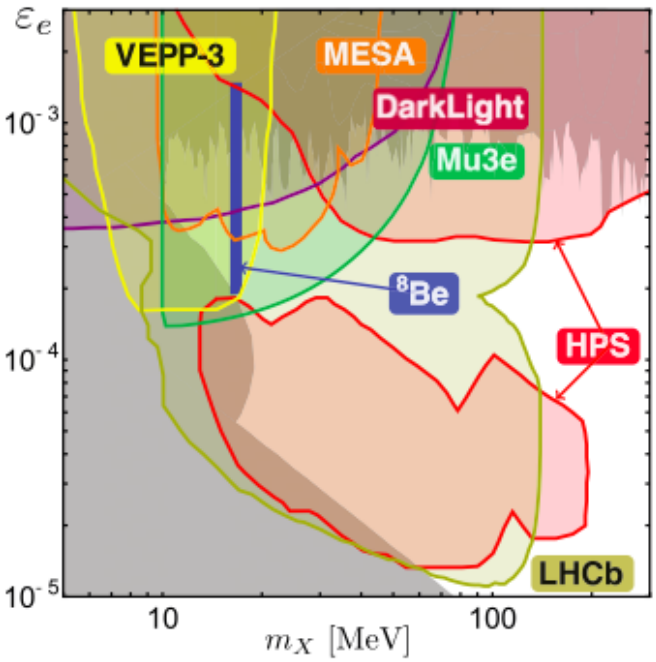

Figure 1: The ^8Be signal region, along with current constraints and projected sensitivities of future experiments in the $(m_x : \epsilon_e)$ plane as discussed in Ref.[2, 3]. For the ^8Be signal, the coupling to electrons is assumed to be in the ranges given by $2 \times 10^{-4} < |\epsilon_e| < 1.4 \times 10^{-3}$.

2 The experiment to search for the decay $X \to e^+e^-$

The method to search for X is the following [57, 5]. If it exists, the bremsstrahlung X could be produced through the reaction

$$e^- + Z \to e^- + Z + X;\ X \to e^+e^- \tag{1}$$

of a high-energy electron scattering off a nuclei in the compact tungsten-scintillator electromagnetic calorimeter (WCAL). The reaction (1) typically occurs within the first few radiation lengths (X_0) of the WCAL detector. The bremsstrahlung X propagates without interatcions and decays in flight into an e^+e^- pair. The detectable signal events are those in which the X decays downstream the WCAL and the veto counter V2 in the decay volume,

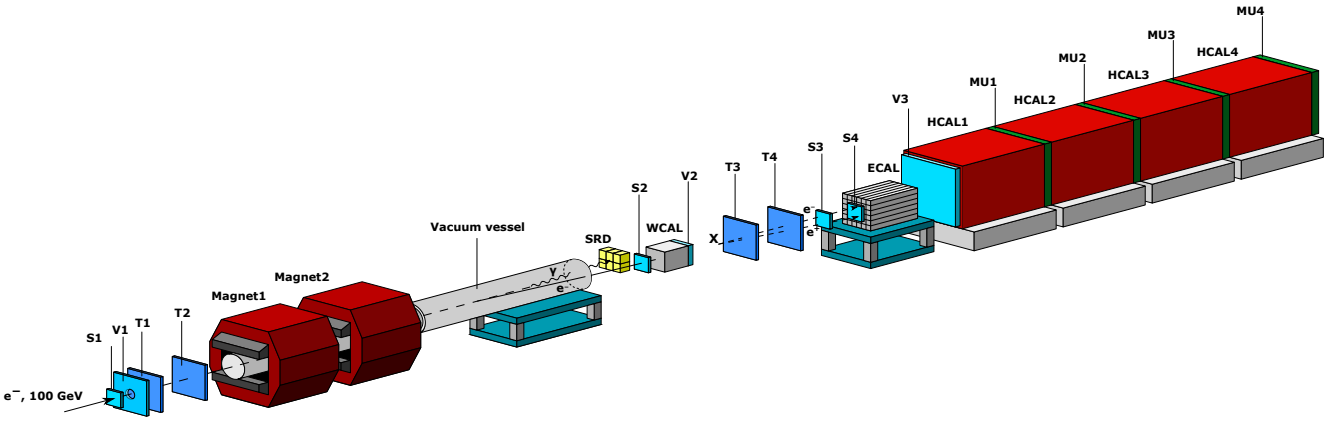

Figure 2: Schematic illustration of the NA64 setup to search for $X \to e^+e^-$ decays with 100 GeV e^- at the H4 beamline. The incident 100 GeV electron energy absorption in the WCAL is accompanied by the emission of bremsstrahlung Xs in the reaction $eZ \to eZX$ of electron scattering off W nuclei. A part of the primary beam energy is deposited in the WCAL by the recoil electron, while the rest of the total energy is transmitted by the X through the WCAL. The X penetrates the WCAL and veto V2 without interactions and decays in flight into a narrow e^+e^- pair, which generates the second electromagnetic shower in the ECAL resulting in the two-shower signature in the NA64 detector. The sum of energies deposited in the WCAL and ECAL is equal to the primary beam energy. The detector is additionally equipped with the massive hadronic calorimeter (HCAL) to enhance its hermeticity.

see Fig.2. A fraction of the primary beam energy $E_1 = E_0 - E_X$ is deposited in the WCAL. The WCAL's downstream part is served as a dump to absorb completely the e-m shower tail. For the radiation length $\lesssim 1$ cm, and the total thickness of the WCAL $\simeq 30$ X_0 (rad. lengths) the energy leak from the WCAL into the V2 is negligibly small. The energy E_X is transmitted trough the "WCAL wall" by the X, and deposited in the second downstream calorimeter, ECAL, by the e^+e^- pair from the X decay, as shown in Fig. 2. At sufficiently high X energies $E_X \gtrsim 30$ GeV, the opening angle $\Theta_{e^+e^-} \simeq M_X/E_X$ of the decay e^+e^- pair is too small to be resolved in two e-m showers in the ECAL, so the pairs are mostly detected as a single electromagnetic shower. At distances larger than $\simeq 5$ m from the WCAL, the distance between the hits is $\gtrsim 5$ mm, so the e^+e^- pair can be resolved in two separated tracks in the T3 and T4 tracker stations.

In October 2016 a short run to test the feasibility for the $X \to e^+e^-$ decays was taken. The experimental setup designed for the search was identical to the one schematically shown in Fig. 2. The experiment employed the 100 GeV e^- beam from the H4 beam line. Two scintillation counter S1 and S2 were used for beam definition, while the other two S3 and S4 were used to detect the e^+e^- pairs. The detector was equipped with a magnetic spectrometer consisting of two MBPL magnets and low material budget tracker. The tracker was a set of two upstream Micromegas (MM) chambers (T1, T2) and two downstream MM and GEM stations each (T3, T4) allowing to measure the incoming e^- direction, and to identify the decay e^+e^- pairs, respectively. The magnets also served as an effective filter rejecting low energy component of the beam. To enhance the electron identification the synchrotron radiation (SR) emitted by electrons was used for their efficient tagging. A 15 m long vacuum vessel between the magnets and the ECAL was installed to minimize absorption of the SR photons detected immediately at the downstream end of the vessel with a SR detector (SRD), which was an array of three PbSc sandwich calorimeters of a very fine segmentation. By using the SRD the initial level of the hadron contamination in the beam $\pi/e^- \lesssim 10^{-2}$ was further suppressed by a factor $\simeq 10^3$. The detector was also equipped with an active target, which is an electromagnetic calorimeter (ECAL) for measurement of the electron energy deposition $E_{ECAL}$with the accuracy $\delta E_{ECAL}/E_{ECAL} \simeq 0.1/\sqrt{E_{ECAL}}$. The ECAL was a

matrix of 6×6 Shashlik-type modules assembled with Pb and Sc plates with wave length shifting fiber read-out. Each module was $\simeq 40$ radiation lengths. Downstream the ECAL the detector was equipped with a high-efficiency veto counter, V3, and a massive, hermetic hadronic calorimeter (HCAL) of $\simeq 30$ nuclear interaction lengths. The HCAL served as an efficient veto to detect muons or hadronic secondaries produced in the $e^- A$ interactions in the target. The HCAL energy resolution was $\delta E_{HCAL}/E_{HCAL} \simeq 0.6/\sqrt{E_{HCAL}}$. Four muon counters, MU1-MU4, located between the HCAL modules were used for the muon identification in the final state.

The occurrence of $X \to e^+e^-$ decays produced in $e^- Z$ interactions would appear as an excess of events with two e-m-like showers in the detector: one in the WCAL, and another one in the ECAL, see Fig. 2, above those expected from the background sources. The signal candidate events have the signature:

$$S_X = \Pi \mathrm{S_i} \times \mathrm{WCAL} \times \overline{\mathrm{V2}} \times \mathrm{ECAL} \times \overline{\mathrm{V3}} \times \overline{\mathrm{HCAL}}, \tag{2}$$

and should satisfy the following selection criteria:

- The starting point of (e-m) showers in the WCAL and ECAL should be localized within first few X_0s.
- The lateral and longitudinal shapes of both showers in the WCAL and ECAL are consistent with an electromagnetic one. The fraction of the total energy deposition in the WCAL is $f \lesssim 0.7$, while in the ECAL it is $(1-f) \gtrsim 0.3$ (see energy spectra in Fig. 9, and discussion below).
- No energy deposition in the V2.
- The signal (number of photoelectrons) in the decay counters S3 and S4 is consistent with the one expected from two minimum ionizing particle (MIP) tracks. At low beam energies, $E_0 \lesssim 30$ GeV, two isolated hits in each counter are requested.
- the sum of energies deposited in the WCAL+ECAL is equal to the primary energy, $E_1 + E_2 = E_0$.

2.1 The SPS H4 secondary beam line

The experiment uses the optimized CERN SPS H4 e^- beam, which is produced in the target T2 of the CERN SPS and transported to the detector in an evacuated beam-line tuned to a freely adjustable beam momentum from 10 up to 300 GeV/c. The typical maximal beam intensity at $\simeq 100$ GeV, is of the order of 5×10^6 e^- for one typical SPS spill with a few 10^{12} protons on target. Note, that a typical SPS cycle for Fixed Target (FT) operation lasts 14.8 s, including 4.8 s spill duration. The maximal number of FT cycles is 4 per minute, however, this number can vary from 1 to 2 per minute.

To provide as maximal as possible coverage of still unexplored area of mixing strength $10^{-4} \lesssim \epsilon_e \lesssim 10^{-3}$ and masses $M_X \simeq 20$ MeV, and also to have realistic beam exposure time, we plan to take measurements with a beam of 100(200) GeV with the total number of accumulated electrons on the WCAL $n_{eot} \gtrsim 10^{11}$ e^-'s. Reaching this goal requires an average beam intensity of $\gtrsim 5 \times 10^6$ e^- per SPS spill. Since there are no special requirements for beam size at the entrance of the detector, which can be within a few cm^2, the beam intensity can be increased by a factor 2 by tuning the beam line optics and collimators up to $\simeq (7-8) \times 10^6$ e^- per SPS spill. It is assumed that the contamination of particles, other than electrons is within a few 10^{-2}. Thus, for an optimistic scenario the total number of electrons accumulated during two weeks of data taking is $n_{eot} \simeq 2 \times 10^{11}$. In a less optimistic case, this number could lay in the range $10^{11} \lesssim n_{eot} \lesssim 2 \times 10^{11}$. Therefore, to accumulate $n_{eot} \gtrsim 10^{11}$ electrons, the data taking period of at least two weeks is requested.

The suppression of any possible background should be at a level of 10^{-12} or below. The advantage of using the H4 beam is that at high energies ($\gtrsim 100$ GeV) the beam is very clean, the contamination of πs in the electron beam is well below 1%. In the analysis presented

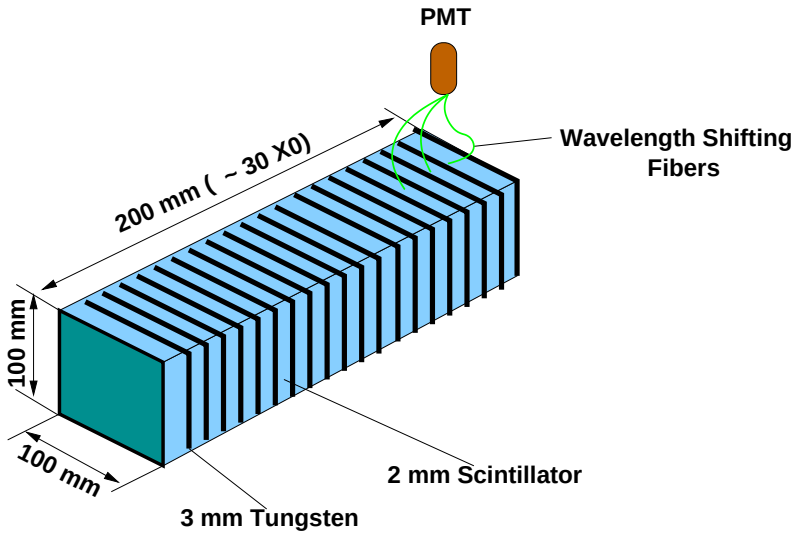

Figure 3: Schematic illustration of a scintillator-fiber-tungsten module consisting of a stack of 3 mm thick tungsten and 2 mm thick scintillator plates. Wavelength shifting fibers pass laterally through the plates and are read out with a photomultiplier.

below, no special treatment was applied to the simulated data to eliminate an eventual pion contamination. The assumed beam purity is $\simeq 10^{-2}$.

A two-stage approach is envisaged for the experiment, incorporating initial experimental test phase in October 2016, followed by the main-goal period of the experiment to reach sensitivity for $\epsilon_e < 1.4 \times 10^{-3}$ in 2017-2018.

2.2 The tungsten - scintillator calorimeter

The choice of the calorimeter type should satisfy the following criteria:

- One of the main requirements for the sensitive search for Xs in the still unexplored parameter space, is to achieve a highly compact design, having a small Moliere radius and a short radiation length. The total length of the detector should be $\lesssim 30$ cm. This implies having the largest amount of absorber possible, consistent with obtaining the required energy resolution.
- The energy resolution should be $\Delta E/E \simeq 15\%/\sqrt{E}$.
- It should be possible to measure the lateral and longitudinal shower shape.
- The e/π rejection should be $\lesssim 10^{-3}$.
- Timing properties should allow high speed data accumulation.
- The radiation hardness must be better then 1000 Gy.

The energy resolution of the WCAL calorimeter as a function of the beam energy was measured to be $\frac{\sigma}{E} = \frac{15\%}{\sqrt{E}} \oplus 3\% \oplus \frac{142\ MeV}{E}$.

To fulfill these design requirements, we adopted a tungsten scintillator sandwich configuration, as shown in Fig. 3. It consists of a standard sandwich arrangement of alternating W absorber and scintillator plates read out with wavelength shifting fibers running laterally through each scintillator plate. Our WCAL module design has high density and represents a compact calorimeter with a small overall module size (roughly 10 square Moliere radius at the front). To improve the e/π rejection factor the WCAL is designed with longitudinal segmentation . One possible option of the calorimeter segmentation is shown in Fig. 3. This design would have the advantage to reading out longitudinal shower profile, by grouping fibers from the first $\simeq 4-5$ X_0 radiation lengths into a separate preshower detector. The WCAL is $\simeq 100 \times 100$ mm^2 in cross section and about 200 mm ($\simeq$30 X_0) long, see Fig. 3.

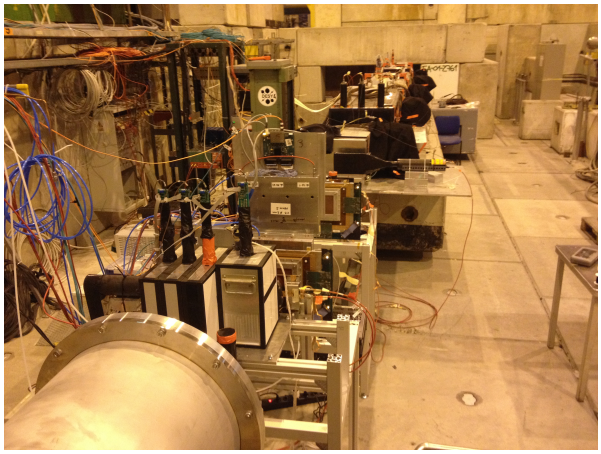

Figure 4: Photograph of the WCAL calorimeter at the H4 beam during the test run in October 2016.

Timing and energy deposition information from each plate has been digitized for each event. In Fig. 4 the photograph of the WCAL calorimeter located at the H4 beam during test run in October 2016 is shown.

To evaluate the basic performance of this design we have carried out a Monte Carlo study by using GEANT4 [59]. For the calorimeter design, the energy resolution requirements are quite stringent and are in the range of a few % for the energy region 30-100 GeV. We studied the WCAL energy resolution for various tungsten plate thicknesses keeping the scintillator thickness constant at 3.0 mm. Fig. 5 gives the results of these simulations. The curves were fit to a parametrization of $\Delta E/E = a/\sqrt{E} + b$ and the results of the fit for the selected W plate thickness of 3.5 mm is $a = 0.15$ and $b = 0.004$. It shows that an energy resolution $\simeq 15\%/\sqrt{E}$ can be achieved with the selected sampling. Note, that only sampling fluctuations and leakage were included in this simulation, therefore the photo-statistics contribution has to be kept small compared to this value.

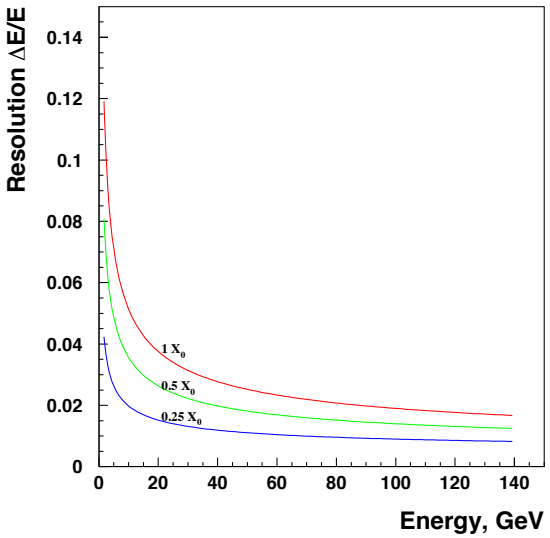

Figure 5: Simulated energy resolution (FWHM) as a function of the incident energy of a calorimeter module configuration shown in Fig. 3 for different absorber plate thicknesses, indicated near the curves. The scintillator plate thickness was kept constant at 3.0 mm for each configuration. Only contributions from sampling fluctuations and energy leakage are included.

We also studied the Moliere radius of this design. The fraction of the energy of a shower contained within a given radius (in terms of radiation length) for a calorimeter with one radiation length sampling and 3 mm scintillator was simulated. For pure tungsten, the Moliere radius is $R_M \simeq 2.6\ X_0 \simeq 9.3$ mm, and is the radius that contains approximately 90% of the shower energy. From the simplified simulation, we can see that in order to absorb nearly 90% of the energy in the counter, its lateral size should be still within roughly one R_M. It was also found that this value is nearly independent of energy from 1-40 GeV. The Moliere radius of this configuration is almost the same as that of pure tungsten, it is larger by about 20%.

2.3 Veto counter

The WCAL calorimeter is followed by the veto counter V2. The veto counter was 10 mm thick made of plastic scintillator with a high light yield of $\simeq 10^2$ photoelectrons per 1 MeV of deposited energy. In the design and construction of this counter the main focus was to maximize the V2 detection efficiency. The typical veto's inefficiency measured for the MIP detection was, conservatively, $\lesssim 10^{-4}$. The main task of the counter is to measure precisely

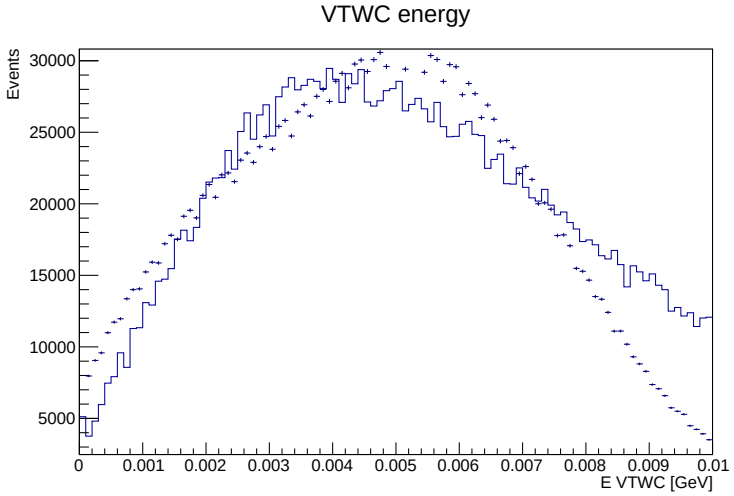

Figure 6: Distributions of energy deposited in the V2 counter from the interactions induced by the 100 GeV e^-'s in the WCAL target and obtained with simulations (histogram) and measured in the October run data (crosses). 1 MIP $\simeq$ 2 MeV deposited energy.

the time and energy deposition of particles escaping the WCAL from the back surface in order to allow the matching with the real electron event and to reject background from hadronic and pile-up events. In Fig. 6 expected distributions of energy deposited in the V2 from the interactions induced by the 100 GeV e^-'s in the WCAL target obtained with simulations and measured in the October run are shown. The difference in distributions, attributed mainly to the difficulties in simulations of the pileup effects at high beam intensities, is taken into account as an additional contribution to the systematic errors for the V2 efficiency to the signal events.

3 The October run 2016

In October run 2016 a short run was taken in order to study the feasibility of the search for the $X \to e^+e^-$ decay with the NA64 setup. For this run,

(i) The detector shown in Fig.2 was assembled.

(ii) The option with two magnets was used for the primary electron identification with the PbSc SRD detector having transverse segmentation.

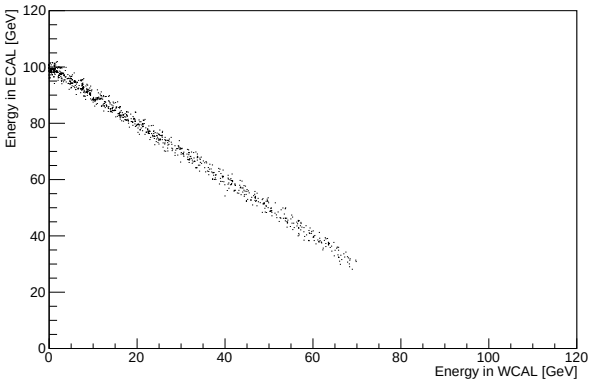

Figure 7: Distribution of simulated signal events on the (E_{WCAL}, E_{ECAL}) plane.

(iii) Several runs at different beam intensities were taken. The number of eot
- $n_{eot} \simeq 0.5 \cdot 10^9$ eot with intensity $\simeq 2 \cdot 10^6$e- / spill.
- $n_{eot} \simeq 1.8 \cdot 10^9$ eot and and intensity $\simeq 3 \cdot 10^6$e- / spill.
-$n_{eot} \simeq 3 \cdot 10^9$ eot and max intensity $\simeq 5 \cdot 10^6$e- / spill.
were recorded.

(iv) Tracker was used to better define the incoming beam and for precise momentum measurements. Two upstream MM1 and MM2 were used to reject large angle tracks and improve collinearity of the incoming beam. Two downstream MM3 and MM4 , as well as GEM1 and GEM 2 stations are planned to be used for the two-track finding from e^+e^- pairs.

(v) To increase the operational efficiency of the experiment the upgraded DAQ system and improved Data Quality Control system were used in the run. The recovery procedures to react on hardware and software failures were also tested.

(vi) Currently, the development of an improved version of the reconstruction and analysis program is in progress, as well as the study of systematic effects, background sources for the final detector configuration in 2017 are ongoing. Preliminary results looks promising.

(vii) Further developments of the DAQ and the analysis program are in progress to ensure a substantial data collection of $n_{eot} \simeq 10^{11}$ events in 2017.

4 Simulation of the X and dark photon production

The production of X boson off nuclei, which is the signal that we search for, was performed by the code described in Ref.[8], compiled as a part of the Geant4 application. We assumed that both electrons and positrons of the electromagnetic shower initiated by the beam electron in the tungsten calorimeter WCAL can produce X with the same cross section. For the visible mode configuration the subsequent $X \to e^+e^-$ decay was simulated. The resulting electron - positron pair was traced by Geant4 in the same way as all other particles. The life time of X depends on its mass and on the mixing constant ϵ_e. We used the mass $m_X = 16.7$ MeV and coupling $\epsilon_e \simeq 10^{-3}$ as a reference point.

Choosing cuts for the signal selection was performed in the following way. In simulations it was observed that in some cases low energy particles from the "signal" e-m shower in the WCAL may still leak through the WCAL rear surface resulting in a signal efficiency drop. To avoid significant reduction of the effciency the cut on V2 being ($\simeq$2 MeV deposited energy, see Fig.6) was chosen to be at $\lesssim 1.3$ MIP. The upper cut on S4 was chosen at the same value for selecting events with at least two charged particles before the ECAL. Distribution

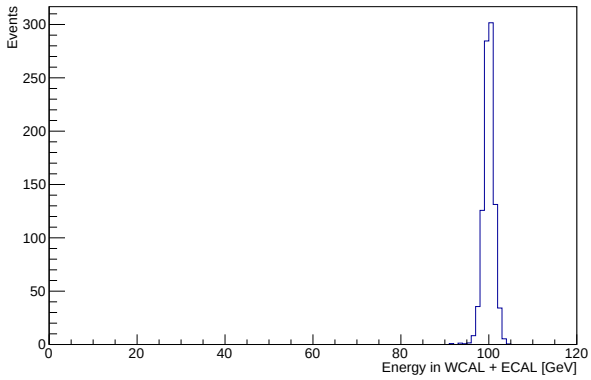

Figure 8: Distribution of the total energy ($E_{WCAL} + E_{ECAL}$) deposited in electromagnetic calorimeters for the simulated signal events.

of simulated signal events in the (E_{WCAL}; E_{ECAL}) plane is shown in Fig.7. The distribution of the total energy deposited in WCAL and ECAL is shown in Fig.8. This total energy deposition is the main variable for the signal selection. Two additional criteria were used.

The yield of X as a function of the WCAL thickness for different values of the threshold on V2 signal is shown in Table1.

Table 1: Yield of the X boson from the W-target

item	no cut on E_{V2}	$E_{V2} < 1.3$MIP	$E_{V2} < 0.7$ MIP
1. Run Oct'16	712	458.6	358
2.Run Oct'16, no gaps, V2 of WCAL size	735	534.7	422
3. 2.+ 5 layers	663	587.2	528
4. 3.+5layers	547	500	477

One can notice that for cases $E_{V2} < 1.3$ MIP and $E_{V2} < 0.7$ MIP the X-yield for the configuration 3) is higher than that of 2), in spite of smaller thickness of the latter. The possible explanation is that the yield is proportional to the product $P(t) \times P(V2)$, where $P(t)$ it the probability for X to escape WCAL and $P(V2)$ is probability for the leak energy to be below the threshold of V2. So the product has the maximum for WCAL thickness around $t \simeq 35\ X_0$.

5 Data analysis and selection criteria

The initial sample for the selection of e^+e^- candidates was obtained from the events satisfying the WCAL trigger,see Table 2. For the analysis we used all available data from the October run 2016. There are several steps in event selection.
At the first step of the analysis with a simple filter we selected events with the following properties:

- event triggering the WCAL should be in time with the Sc trigger;
- the usual quality cuts: bad runs, unused hits, etc...should be satisfied; The maximal allowed error of the total event energy measurement is in this case $\simeq 1.5E_0$.
- event should have one good quality track at the entrance, with the number of hits not more than 2 each per MM plane.
- the selected events were also required to be in time with the trigger scintillator counters.

- No MIP signals in V2 and V3. Since energy deposited in the Veto played a crucial role in the analysis, only events with the energy deposition as listed in Table 1 were accepted.
- no activity in HCAL modules.

The purpose of these cuts is to clean up the initial sample. Finally the $X \to e^+e^-$ candidate events were selected with the following criteria:

(i) no requirement of an oppositely charged particles in the pair or presence of a track identified as a positron, i.e. the behavior of the e^+e^- tracks with a narrow angle must be consistent with the one expected from a single electron track

(ii) e^+, e^- identification by the ECAL shower shape, $\chi^2 < 8$

(iii) energy in the hadronic calorimeter < 0.4 GeV. This cut serves as HCAL veto and was cross-checked with the random trigger and Monte Carlo studies.

(iv) Muon HCAL veto: no muons in the final state.

(v) the starting point of (e-m) showers in the ECAL should be localized within first few X_0s.

(vi) the lateral and longitudinal shapes of the ECAL shower is consistent with the electromagnetic one.

(vii) The fraction of the total energy deposition in the WCAL is $f \lesssim 0.7$, while in the ECAL it is $(1-f) \gtrsim 0.3$ (see Fig.9 and discussion below).

(viii) no energy deposition in the V2 (<1.5 MIP) and V3(< 0.5 MIP).

(ix) the signal (number of photoelectrons) in the decay counter S4 is consistent with the one expected from two minimum ionizing particle (mip) tracks: S4 > 1.5 MIP. For low energies of the e^+e^- pairs with $E_{e^+e^-} \lesssim 30$ GeV two isolated hits in the M3 and M4 could be requested (to be studied).

(x) the sum of energies deposited in the WCAL and ECAL is equal to the primary energy, $E_{WCAL} + E_{ECAL} = E_0$ within the energy resolution for events with maximum energy deposited in the cell (3;3) of the ECAL.

In total out of about 2.6×10^6 events recorded, see Table 2, only 16 events passed the above search criteria, and no candidate events satisfying $E_{WCAL} + E_{ECAL} > 92$ GeV requirement were found. The evolution of selection efficiency is shown in Table 2.

Below several comments for the further study are presented

(i) Efficiency of the e^+e^- pair reconstruction

In order to check the efficiency of e^+e^- pairs reconstruction in NA64, reconstructed dimuon pairs from the purely QED reaction $e^-Z \to e^-Z\gamma; \gamma \to \mu^+\mu^-$ in the WCAL target were used. The experimental signature of a dimuon event is a clean double MIP signal in the HCAL modules in the very forward direction, typically in the HCAL central cells, accompanied by the dimuon signal in the tracker. The efficiency for signal pairs in the energy range predicted by the simulations, was estimated by studying the detection efficiency of those dimuon pairs. An estimate shows that, as expected, the efficiency is quite high, $\gtrsim 70-80\%$, however further study is required, in particular for better alignment of detectors in the downstream part of the setup.

(ii) $WCAL \cdot \overline{V2} \cdot S_2$ trigger efficiency study. The $WCAL \cdot \overline{V2} \cdot S_2$ trigger efficiency was estimated with the same process of $\mu^+\mu^-$ pair production in the target.

The flow of efficiency numbers is shown in Table 2.

6 Results from the October run 2016

The distribution of the selected candidate events on the (E_{WCAL}, E_{ECAL}) plane from the October 2016 run is shown in Fig. 10. The dashed band shows the signal box region

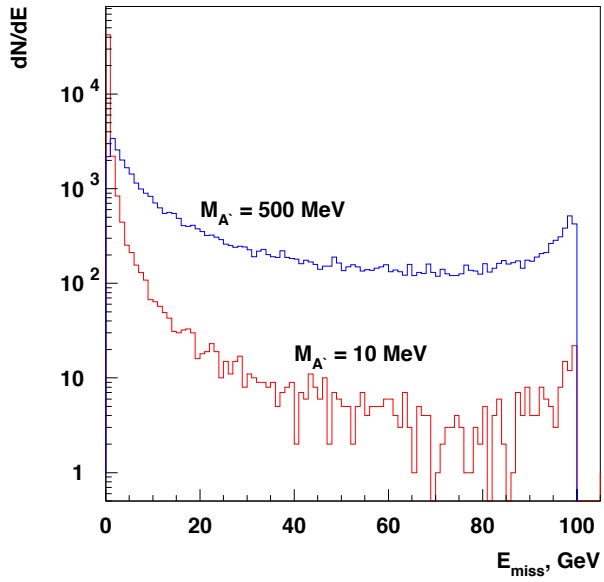

Figure 9: The X emission spectrum from 100 GeV electron beam interactions in the Pb target calculated for $m_X = 10$ MeV and $m_X = 500$ MeV. The spectra are normalized to about the same number of events.

corresponding to $E_{WCAL} + E_{ECAL} = E_0$. The distribution of the total energy deposited in WCAL and ECAL is shown in Fig.11. This distribution can be compared with the one shown in Fig.12, where the distribution of energy deposited in the WCAL by 100 GeV e^- is shown. This plot was used to determine roughly the size of the signal box $90 \lesssim E_{tot} \lesssim 110$ GeV. Note, that the total energy deposition E_{tot} is the main variable for the signal selection. Two additional criteria were used for the signal selection. The first is the requirement that the ECAL cell with the maximal energy deposition is the cell (3,3), the cell where the beam enters the ECAL when WCAL is not installed. The signal simulation showed that the efficiency of this requirement for the signal is higher than 99%. The second requirement is of no energy (<0.8 MIP) in VETO, it ensures that there are no hadrons after the WCAL.

We observe no events which pass our search criteria and selection cuts. The number of expected background events is approximately 0.3. The largest contribution to the background is expected either from the high-energy punch-trough photons or from the hadronic

Table 2: Efficiency for the $X \to e^+e^-$ decay event selection in simulations and data. Also flow of the accepted numbers for the simulated single 100 GeV electron selection is shown.

item	Simulations $m_X = 16.7$ MeV n_{acc} signal	Data n_{acc} candidates	Single e^- n_{acc}
Initial number of events	2000 (with $E_X > 20$ GeV)	2.6×10^6	10^5
Trigger WCAL$\lesssim$ 70 GeV	1720	2.5×10^6	16
Veto V2 cut < 1.3 MIP	1132	8.5×10^5	1
S4> 1.4 MIP	1131	6.3×10^5	0
Veto V3< 0.8 MIP	1065	4×10^3	
ECAL max in cell (3,3)	1063	16	
ECAL shower shape, χ^2	not used	not used	
$E_{WCAL} + E_{ECAL} > 92$ GeV	1062	0	

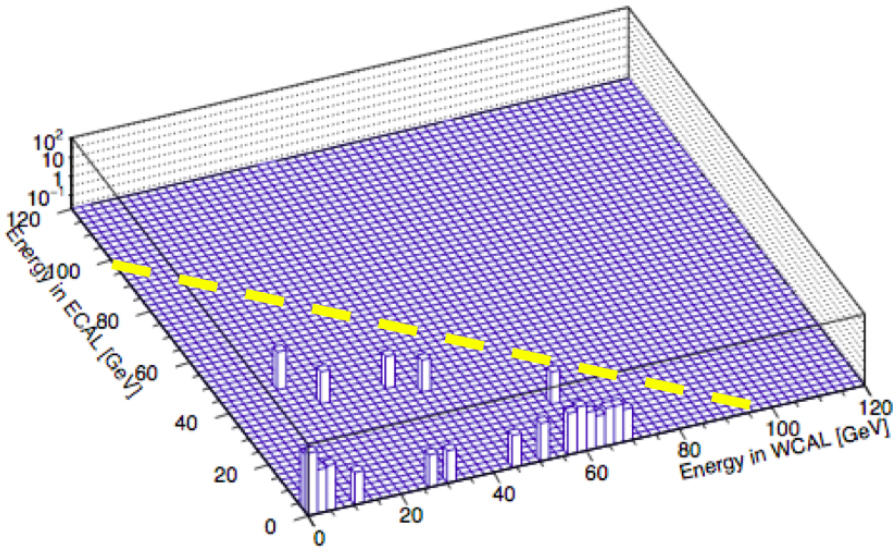

Figure 10: Selected event distribution on the (E_{WCAL}, E_{ECAL}) plane from the October 2016 run. The band shows the signal box region corresponding to $E_{WCAL} + E_{ECAL} = E_0$.

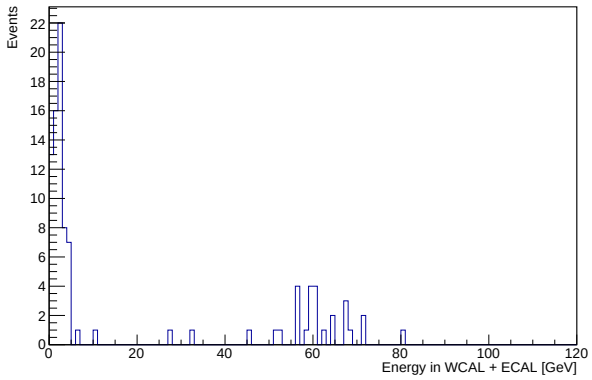

Figure 11: Selected event distribution in the $E_{tot} = E_{WCAL} + E_{ECAL}$ from the October 2016 run. The signal box region corresponding to $90 \lesssim E_{tot} \lesssim 110$ GeV.

interactions with large π^0 component and little charged hadron activity.

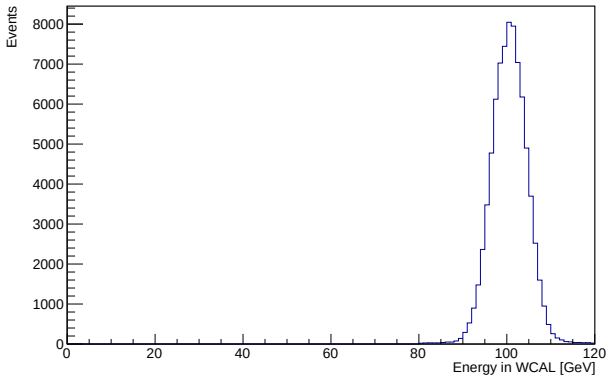

Figure 12: Distribution of energy deposited in the WCAL by 100 GeV e^- from the October run 2016. The signal box region is roughly defined to be $90 \lesssim E_{tot} \lesssim 110$ GeV.

After application of all these cuts - no e^+e^- candidates remained. In Fig. 10 the remaining

event distribution on the (E_{WCAL}, E_{ECAL}) plane from the October run 2016 is presented. It is seen that after the application of all cuts no e^+e^- candidate events are left in the data in the signal band $E_0 = E_{WCAL} + E_{ECAL}$. The 1D-distribution of variable $E_{tot} = E_{WCAL} + E_{ECAL}$ is shown also in Fig.11. Background events are distributed in the low energy part of the plot and most of them were identified as hadronic secondaries from the electroproduction in the WCAL target and no candidate events left in the $X \to e^+e^-$ signal region $90 \lesssim E_{tot} \lesssim 110$ GeV which was approximately defined from the plot of Fig.12. The 90% C.L. upper limit for the production of the X can be calculated by using the following relation:

$$N_{X \to e^+e^-} < N^{90\%}_{X \to e^+e^-} \tag{3}$$

where $N^{90\%}_{X \to e^+e^-}$ is the 90% C.L. upper limit for the expected number of signal events, calculated according to ref. [8].

7 Background

The largest contribution to the background is expected mainly from i) high-energy punch-through photons from the first and second e-m shower generations; ii) single π^0 production in the charge-exchange reactions of beam pions at the last W plates of the WCAL calorimeter.

7.1 γ, e^- - punchthrough level and its direct measurements

- The leak of the primary electron energy into the ECAL, could be due to the bremsstrahlung process $e^-Z \to e^-Z\gamma$, when the emitted photon carries significant fraction of initial energy, $E_\gamma \gtrsim 0.3E_0$, while the final state electron with lower energy $E_{e^-} \lesssim 0.7E_0$ is absorbed in the WCAL. The bremsstrahlung photon could punch through the WCAL and V2 without interactions, and produce an e^+e^- pair in, e.g. S3, which deposit all its energy in the ECAL. The photon could also be absorbed in a photonuclear reaction occurring in the WCAL and resulting in, e.g. an energetic leading secondary neutron.

  For the first case, to suppress this background, one has to use the WCAL of enough thickness, and as low veto energy threshold as possible. Assuming that the primary interaction vertex is selected to be within first few X_0s, for the total remaining WCAL+V2 thickness of $L_{WCAL} \simeq 30\ X_0$, the probability for a photon to punch through both WCAL and V2 without interaction is roughly $P_{pth} \simeq P_\gamma \cdot exp(-\lambda L_{WCAL}) \simeq 3\times10^{-11}$, where $\lambda = 7/9X_0$ and conservatively we take the probability for the bremsstrahlung photon emission with $E_\gamma \gtrsim 0.3E_0$ in the first or/and second shower generation to be $P_\gamma = 1$. Taking into account the probability for the punch-trough γ conversion in downstream material $P_c \lesssim 10^{-2}$ (the thickness of S3 is 3 mm, and hence $P_c \lesssim 10^{-2} = 3/400$ for plastic scintillator, one may conclude, that this background is expected to be at a negligible level. For the second case, an estimation results in a even similar background level. This conclusion strongly depends on the predicted flux of punch-through γ's. To predict this flux accurately is quite difficult. E.g. a precise knowledge of the target material composition, and very time consuming simulations are required. So, this flux is supposed to be estimated directly from the data as explained below.

- Punch-through primary electrons, which penetrate the WCAL and V2 without depositing much energy could produce a fake signal event. It is found that this is also an extremely rare event. In Table 2 just for completeness a flow numbe of simulated 10^5 electron events is shown.

To evaluate the background in the signal region from the punch-through γ's, events selected with the neutral trigger, i.e. with requirements of no signal in V2, S2, and S4 counters, were studied. In Fig. 13 the selected event distribution in the $(E_{WCAL}; E_{ECAL})$ plane from the October run 2016 is shown. No events are observed in the signal region indicated with a yellow band corresponding to the condition $E_0 = E_{WCAL} + E_{ECAL}$. This

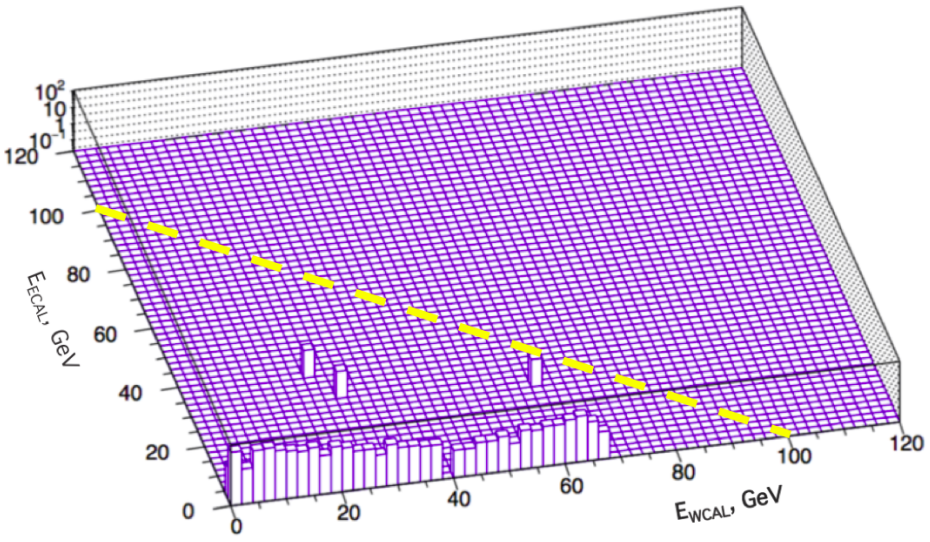

Figure 13: Selected "neutral trigger" event distribution in the $(E_{WCAL}; E_{ECAL})$ *plane from the October run 2016. The yellow band shows the signal box region corresponding to* $E_{WCAL} + E_{ECAL} = E_0$.

allows to set a 90% C.L. upper limit $P_{pth} < 10^{-9}$/eot on the probability to observed a single punch-through event with energy $E^{\gamma}_{pth} \gtrsim 50$ GeV per eot, which is consistent with the above considerations.

7.2 Hadronic background

The hadronic beam-related background can be due to a beam particle misidentified as an electron. This background is caused by some pion, proton and muon contamination in the electron beam. One could perform independent direct measurements of its level with the same setup by using pion and muon beams of proper energies. For this purpose the primary beam is tuned to pions. The muons can be selected by putting thick absorber on the primary beam line.

- The first source of this type of background could be due to the

$$p(\pi) + A \to n + \pi^0 + X,\ n \to \text{ECAL} \tag{4}$$

reaction chain: i) an incident hadron produces a neutral pion with the energy $E_{\pi^0} \lesssim 0.1E_0$ and an energetic leading neutral hadron, e.g. neutron, carrying the rest of the energy of the primary collision with the nucleus (A,Z), ii) the neutral pion decays $\pi^0 \to 2\gamma$ generating an e-m shower in the WCAL, while iii) the neutron penetrates the rest of the WCAL and the veto counter V2 without interactions, scatters in the counter S1, producing low energy secondaries and deposits all its energy in the ECAL. The probability for such a reaction chain to occur can be estimated as

$$P_{p(\pi)} \simeq f_{p(\pi)} \cdot P_{\pi^0 n} \cdot P_{S1} \cdot P_n\,, \tag{5}$$

where $f_{p(\pi)}$, $P_{\pi^0 n}$, P_{S1}, P_n are, respectively, the level of the admixture of hadrons in the primary beam, $P_{p(\pi)} \lesssim 10^{-2}$, the probability for an incoming hadron to produce the $\pi^0 n$ pair in the WCAL, $P_{\pi^0 n} \simeq 10^{-4}$, the probability for the neutron to interact in S1, $P_{S1} \simeq 10^{-3}$, and the probability for the leading n to deposit all its energy in the ECAL, $P_n \simeq 10^{-3}$. This results in $P \lesssim 10^{-12}$. The probability for neutral hadrons to interact in the S1 of thickness $\simeq 1$ mm, or $\simeq 10^{-3}$ nuclear interaction length, can be reduced significantly, down to $P_{S1} \simeq 10^{-4}$, by replacing it, e.g. with a wire chamber counter. This leads to $P \lesssim 10^{-13}$. At low energies $E_0 \lesssim 30$ GeV, the requirement to have two hits in the S1 would suppress the background further.

Note, that the cross section for the reaction $p(\pi) + A \to \pi^0 + n + X$, with the leading neutron in the final state, has not yet been studied in detail for the wide class of nuclei and full range of hadron energies. To perform an estimate of the $P_{\pi^0 n}$ value, we use data from the ISR experiment at CERN, which studied leading neutron production in pp collisions at $\sqrt{s}$ in the range from 20 to 60 GeV [62, 63]. For these energies the invariant cross sections, obtained as a function of x_F (Feynman x) and p_T, were found to be in the range $0.1 \lesssim E\frac{d^3\sigma}{d^3p} \lesssim 10$ mb/GeV^2 for $0.9 \lesssim x_F \lesssim 1$ and $0 \lesssim p_T \lesssim 0.6$ GeV [62]. Taking these results into account, the cross sections for leading neutron production in our energy range are estimated by using the Bourquin-Gaillard formula, which gives the parametrized form of the invariant cross section for the production in high-energy hadronic collisions of different hadrons over the full phase-space, for more details see, e.g. [64]. The leading neutron production cross sections in $p(\pi)A$ collisions are evaluated from its linear extrapolation to the target atomic number.

In another case, the leading neutron could interact in a very downstream part of the veto counter producing leading π^0 without being detected. The π^0 decays subsequently into 2γ or $e^+e^-\gamma$. The background from this events chain is also estimated to be very small.

- The fake signature S_X arises when the incoming pion produces in a very upstream part of the WCAL a low energy neutral pion(s), then it escapes detection in the V2 counter due to its inefficiency, and either deposits all its energy in the ECAL, or decays in flight in the DV into an $e\nu$ pair with the subsequent decay electron energy deposition in the ECAL. In the first case, also relevant to protons, an analysis similar to the previous one, shows that this background is expected to be at the level $\lesssim 10^{-13}$. In the second case, taking into account the probability for the $\pi \to e\nu$ decay in flight, and that the electron would typically have about one half of the pion energy, results in a suppression of this background to the level $< 10^{-15}$. For both cases, taking into account the probability for pion or decay electron, to mimic the double MIP (two tracks) signature in the downstream part of the detector, $\lesssim 10^{-2}$ results in further suppression of this background source.

The overall probability of the fake signal produced by an incoming hadron is estimated to be $P_{p(\pi)} \lesssim 10^{-13}$ per incoming electron. Another type of background is caused by the muon contamination in the beam.

7.3 Muon background

- The muon could produce a low energy bremsstrahlung photon in the WCAL, which would be absorbed in the detector, then penetrates the V2 without being detected, and after producing signals in the S1 and S2 counters, deposit all its energy in the ECAL through the emission of a hard photon:

$$\mu + Z \to \gamma + \mu + Z,\ \mu \to \text{ECAL}\,. \tag{6}$$

The probability for the chain (6) is estimated to be $P \lesssim 10^{-14}$. Similar to (4), this estimate is obtained assuming that the muon contamination in the beam is $\lesssim 10^{-2}$, the probability for the muon to cross the V2 counter without being detected is $\lesssim 10^{-4}$, and the probability for the μ to deposited all its energy in the ECAL is $\lesssim 10^{-7}$. Here, it is also taken into account that the muon should stop in the ECAL calorimeter completely to avoid being detected in the counter V2. An additional suppression factor arises from the requirement to have two-mip's signal in the decay counters.

- One more background source can be due to the event chain

$$\mu + Z \to \mu + \gamma + Z,\ \mu \to e\nu\nu, \tag{7}$$

when the incoming muon produces in the initial WCAL part a low energy bremsstrahlung photon, escapes detection in the counter V2, and then decays in flight in the DV into

Table 3: Expected contributions from different background sources estimated for the beam energy 100 GeV (see text for details).

Source of background	Expected level
punchthrough γs	$< 10^{-10}$
hadronic reactions	$\lesssim 2 \times 10^{-13}$
μ reactions	$\lesssim 10^{-14}$
accidentals	$\lesssim 10^{-14}$
Total (conservatively)	$< 10^{-10}$

$e\nu\nu$. There are several suppression factors for this background: i) the relatively long muon lifetime resulting in a small probability to decay, ii) the presence of two neutrinos in the μ decay. The energy deposition of decay electrons in the ECAL is typically significantly smaller than the primary energy E_0, and iii) the requirement to have double mip energy deposition in the beam counters S1 and S2. All these factors lead to the expectation for this background level to be at least $\lesssim 10^{-14}$.

- A random superposition of uncorrelated events during the detector gate time could also results in a fake signal. Taking into account the selection criteria of signal events results in a the small number of these background events $\lesssim 10^{-14}$.

The overall probability of the fake signal from muons is estimated to be $P_\mu \lesssim 10^{-14}$ per incoming electron, and the accidental background is below $\lesssim 10^{-14}$.

In Table 3 contributions from all background sources are summarized for the beam energy of 100 GeV. The dependence on the energy is rather weak. The total background level is conservatively $\lesssim 10^{-10}$, and is dominated by the high-energy γ punch-throughs with a possible contribution from an admixture of hadrons in the electron beam. Thus, a search accumulating up to $\simeq 10^{11}$ e^- events, is expected to be either background free, or with a small background which is well under control.

8 Sensitivity of the experiment

To estimate the sensitivity of the proposed experiment a simplified feasibility study based on GEANT4 [59] Monte Carlo simulations has been performed for 100 (and also 150) GeV electrons. The energy threshold in the WCAL is taken to be 0.5 GeV. The reported further analysis also takes into account materials in the downstream part of the beamline.

The significance of the $X \to e^+e^-$ decay discovery with the described detector scales as [65, 66]

$$S = 2 \cdot (\sqrt{n_X + n_b} - \sqrt{n_b}) \,, \tag{8}$$

where n_X is the number of observed signal events (or the upper limit of the observed number of events), and n_b is the number of background events.

For a given number of electrons on the target $n_{eot} = n_e \cdot t$ (here, n_e is the electron beam intensity and t is the experiment running time), the length of the target $L_{WCAL} \simeq 200$ mm, and X flux dn_X/dE_X, the expected number of $X \to e^+e^-$ decays occurring within the fiducial volume of the DV with the subsequent energy deposition in the ECAL calorimeter, located at a distance $L \simeq 3$ m from the X production vertex is given by

$$n_X \sim n_e t \int A \frac{dn_X}{dE_X} exp\big(-\frac{L_{WCAL} M_X}{p_X \tau_X}\big) \big[1 - exp\big(-\frac{L M_X}{p_X \tau_X}\big)\big] \frac{\Gamma_{e^+e^-}}{\Gamma_{tot}} \varepsilon_{e^+e^-} dE_X dV \,, \tag{9}$$

where p_X is the X momentum, τ_X is the X lifetime at the rest frame, $\Gamma_{e^+e^-}$, Γ_{tot} are the partial and total X-decay widths, respectively, and $\varepsilon_{e^+e^-} (\simeq 0.9)$ is the e^+e^- pair reconstruction efficiency. The flux of Xs produced in the process (1) is calculated by using the X

production cross section in the $e^- Z$ collisions from Ref. [27]. The acceptance A of the ECAL calorimeter is calculated tracing Xs produced in the WCAL to the ECAL, and is close to 100%.

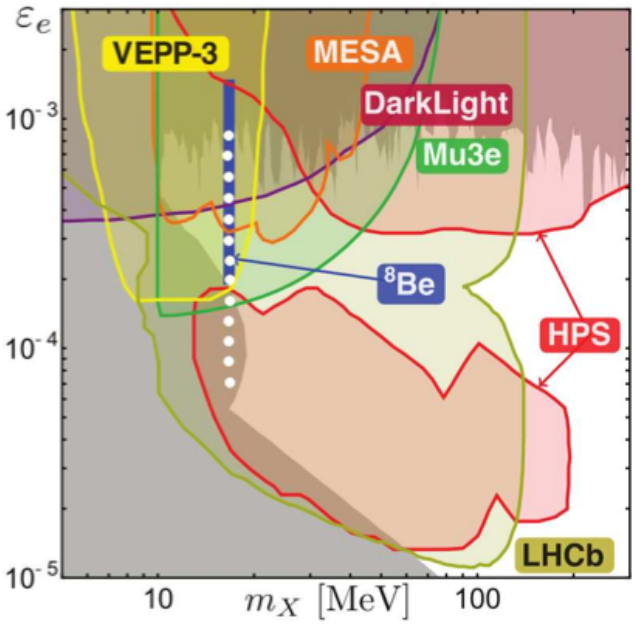

Figure 14: The ^{8}Be signal region, along with current constraints and projected sensitivities of future experiments in the $(m_x : \epsilon_e)$ plane as discussed in Ref.[2, 3]. The white points indicate expected 90% C.L. exclusion areas in the $(m_X; \epsilon_e)$ plane from NA64 for the accumulated statistics of 10^{11} eot at 100 GeV. For the ^{8}Be signal, the coupling to electrons can be in the range $2 \times 10^{-4} < |\epsilon_e| < 1.4 \times 10^{-3}$, while the excluded area is $7 \times 10^{-5} < |\epsilon_e| < 0.9 \times 10^{-3}$

If no excess events are found, the obtained results can be used to impose bounds on the $\gamma - X$ mixing strength as a function of the dark photon mass. Taking Eqs. (8) and (9) into account and using the relation $n_X(M_X) < n_X^{90\%}(M_X)$, where $n_X^{90\%}(M_X)$ is the 90% C.L. upper limit for the number of signal events from the decays of the X with a given mass M_X one can determine the expected 90% C.L. exclusion area in the $(M_X; \epsilon_e)$ plane from the results of the experiment. For the background free case *($n_X^{90\%}(M_X) = 2.3$ events)*, the exclusion regions corresponding to accumulated statistics 10^{11} eot at 100 GeV are shown in Fig. 14. One can see, that these exclusion areas are complementary to the ones expected from the planned APEX (full run), HPS and DarkLight experiments, which are also shown for comparisonn [2, 3]. In Fig.15 and 16, the number of observed events from the $X \to e^+e^-$ decays as a function of coupling ϵ_e for different e^- beam energies and accumulated number of events are shown. In Fig.16 the curves are obtained after parameterization of the n_x vs ϵ_e dependence shown in Fig.15 with the function

$$f(\epsilon_e) = \alpha \epsilon_e^2 exp(-\beta \epsilon_e^2) \tag{10}$$

where the first term $\alpha\epsilon_e^2$ describes the X yield from the reaction $eZ \to eZX$ in the WCAL, while the second term $exp(-\beta\epsilon_e^2)$ corresponds to the fraction of Xs decaying outside of the WCAL. The fit gives $\alpha \simeq 8 \times 10^8$, $\beta \simeq 6.7 \times 10^6$. In Fig.16 the coupling ϵ_e range for ^{8}Be excess is also shown. The horizontal line indicates the level of $n_X = 2.3$ events above which the values of the coupling ϵ_e are excluded in case of no signal observation.

The statistical limit on the sensitivity of the proposed experiment is proportional to ϵ_e^2. Thus, it is important to accumulate a large number of events. As one can see from Eq. (9), the obtained exclusion regions are also sensitive to the choice of the length L' of the calorimeter WCAL, which should be as short as possible. As discussed in Sec. 2.1, assuming the maximal

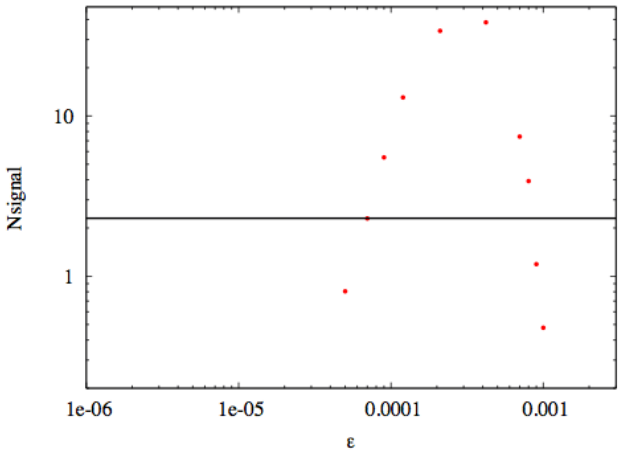

Figure 15: The number n_X of observed events from the $X \to e^+e^-$ decays as a function of coupling ϵ_e calculated for several values of the coupling ϵ_e indicated by red points. The horizontal line indicates the level of $n_X = 2.3$ events above which the values of the coupling ϵ_e are excluded in case of no signal observation.

secondary H4 beam rate $n_e \simeq 5 \times 10^6$ e^-/spill at $E_0 \simeq 100 - 150$ GeV, we anticipate $\simeq 10^{11}$ collected e^-s during $\simeq$ 2 weeks of running time for the experiment. Note, that since the decay time of the scintillating-fiber light signal is $\tau \lesssim 50$ ns, the maximally allowed electron counting rate in order to avoid significant pileup effect is, roughly $\lesssim 1/\tau \simeq 10^7$ e^-/s. This is well compatible with the maximal beam rate during the 4.8 s spill, which is expected to be $\lesssim 10^7/4.8s \simeq 2 \times 10^6$. To minimize dead time, one could use a first-level trigger rejecting events with the ECAL energy deposition less than, say, the energy $\simeq 0.9E_0$ and, hence, run the experiment at a even higher rate.

In the case of the signal observation, to cross-check the result, one could remove the decay vessel DV and put the calorimeter ECAL behind the WCAL. This would not affect the main background sources and still allow the Xs production, but with their decays upstream of the ECAL calorimeter being suppressed. The distributions of the energy deposition in the WCAL and ECAL in this case would contain mainly background events, while the signal level from the decays $X \to e^+e^-$ should be reduced. The background can also be independently studied with the muon and pion beams of the same energy. The evaluation of the X mass value could be obtained from the results of measurements at different distances L and beam energies. Finally note, that the performed analysis for the sensitivity of the proposed experiment may be strengthened by more accurate and detailed simulations of the H4 beam line and concrete experimental setup.

We also plan to install and test several straw tube chambers (STC) with the straw diameter of 6 mm (2 STCs) and 2 mm (2 STCs). These STCs have been designed with the aim to distinguish and reconstruct two close tracks from the visible X decay mode, such as $X \to e^+e^-$xs.

Compared with the setup of 2016, the following main modifications will be used in 2017.

9 Plans for 2017

(i) To test the intensity of the e^- beam up to $\gtrsim 7 \cdot 10^6$ e^-/ spill

(ii) In October'16 the detector was tested up to $5 \cdot 10^6$ e^-/ spill or $\simeq 10^{10}$ e^-/ collected during one day for the "normal" SPS operation with ∼2 supercycles per minute. Good performance of the setup was demonstrated. With intensity $\sim 7 \cdot 10^6$ e^-/ spill accumulation $\simeq 10^{11}$ e$^-$ during one week - 10 days of running is feasible.

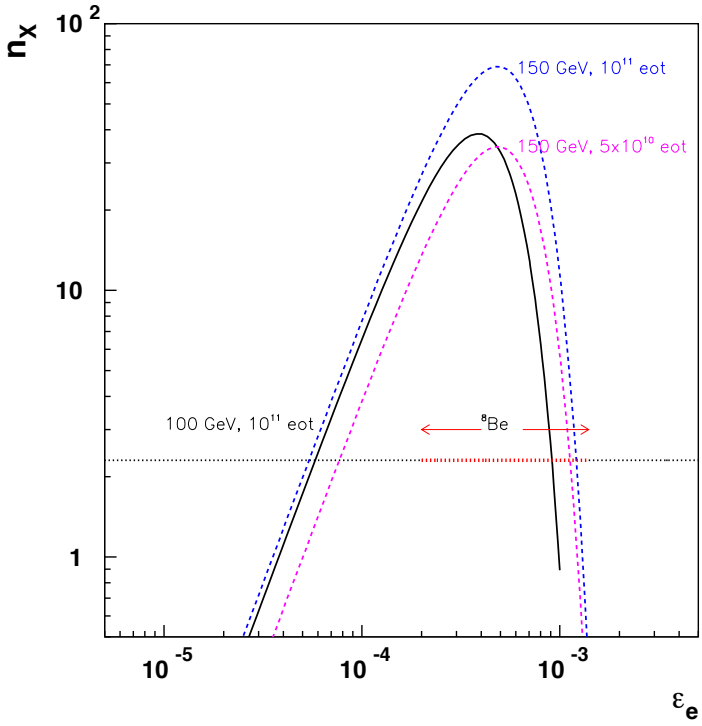

Figure 16: The number of observed events from the $X \to e^+e^-$ decays as a function of coupling ϵ_e for different e^- beam energies and accumulated number of events. The curves are obtained after parameterization of the n_x vs ϵ_e dependence shown in Fig.15 The coupling ϵ_e range for ^8Be excess is also shown. The horizontal line indicates the level of $n_X = 2.3$ events above which the values of the coupling ϵ_e are excluded in case of no signal observation.

To increase the overall signal efficiency and improve background rejection the following upgrade of the setup is foreseen:

(iii) Tracker: additional number of the MM, GEM, ST stations.

(iv) Two fast beam hodoscopes.

(v) SRD: use of transverse segmentation of PbSc SRD detector with upgraded readout.

(vi) Zero-angle veto to suppress events accompanied by bremsstrahlung photons from the beam interactions in the upstream part of the H4 beamline, e.g. in residual gas, vacuum windows, beam collimators, etc..

(vii) Large Veto in front of the ECAL to reject low energy electrons.

(viii) Upstream Sc counter to improve beam divergence.

(ix) The QED $\mu^+\mu^-$ pairs observed for from high-energy γ-conversion is a rare process and is very useful as a reference channel for signal reconstruction efficiency and possible systematic errors. It is an important benchmark for comparison and cross check of Data and MC. The HCAL module calibration and monitoring during the data taken period is important and should be improved.

(x) Probably the most important current task is to show that the signal to background ratio in the signal search is not damaged by the addition and modification of the detectors. Currently we are focusing on further development of the reconstruction and analysis program. At present, the manpower does appear to be adequate to complete the task in a timely manner. We are convinced that our plans to complete conclusive analysis by June are realistic. And first results on either observation of the signal or exclusion area derivation will be available.

(xi) Installation already requires about 2 days, testing the setup plus calibration about three days more. In 2017 more complex setup is expected to be used, resulting in possible increase of time needed for installation, alignment and calibration. A permanent location at H4 would be useful to avoid loss of the beam time.

10 Competition

The theoretical status of the ^{8}Be anomaly has been discussed by J.Feng in his talk at the recent CERN-EPFL-Korea Theory Institute "New Physics at the Intensity Frontier". It will be also extensively discussed at a forthcoming workshop focusing on potential new small-scale projects in the U.S. Dark Matter search program, which will be held at the University of Maryland, College Park March 23-25, 2017. According to the agenda a few talks devoted to the possible searches for Be excess events are foreseen.

In Fig.1, one can see that experiments such as MESA, Dark Light, VEPP-3 potentially could probe the X parameter space. Among them probably the Dark Light experiment at JLab is the most serious competitor. The current status of the DarkLight experiment at Jefferson Laboratory is not precisely known, but they had a run in 2016. They are sensitive to short lived dark photons in the mass range 10 to 100 MeV/c2. The Dark Light techniques is based on precisely measured electron proton scattering using the 100 MeV electron beam of intensity 5 mA at the Jefferson Laboratory energy recovering linac incident on a windowless gas target of molecular hydrogen. The experiment is intended to run at least a couple of years.

Another experiment aiming at the study of the $X \to e^+e^-$ decay modes by exploiting the new Mainz Energy Recovering Superconducting Accelerator (MESA, see Fig. 1) in Mainz. The plan is to reach a sensitivity down to the level of $\epsilon \simeq 10^{-3}$ in the mass range $m_X \lesssim 20$ MeV in about two years. This is a competitor to NA64 although their plan is to be commissioned in 2020. Here, however, one should take into account the LS2 period 2019-2020 at LHC during which the NA64 also will not run.

11 Conclusion

We propose new measurements dedicated to the sensitive search for the $X \to e^+e^-$ decay of a new short-lived neutral boson X with a mass 16.7 MeV and coupling to electrons in the range $2 \times 10^{-4} < \epsilon_e < 1.4 \times 10^{-3}$ which could explain an excess of e^+e^- pairs observed in the excited ^{8}Be* nucleus transitions.

If such X's exist, they could be searched for in a light-shining-through-a-wall experiment with a high energy electron beam. The electron energy absorption in a calorimeter (WCAL) is accompanied by the emission of bremsstrahlung X's in the reaction $eZ \to eZX$ of electrons scattering off a nuclei due to the $e - X$ coupling. A part of the primary beam energy is deposited in the WCAL, while the rest of the energy is transmitted by the X through the "WCAL wall" and deposited in another downstream calorimeter ECAL by the e^+e^- pair from the $X \to e^+e^-$ decay in flight. Thus, the X's could be observed by looking for an excess of events with the two-shower signature generated by a single high energy electron in the WCAL and ECAL. A proposal to perform such an experiment to probe the still unexplored area of the coupling strength $10^{-4} \lesssim \epsilon_e \lesssim 10^{-3}$ and mass $m_X = 16.7$ MeV by using 100-150 GeV electron beams from the CERN SPS is presented. The search can provide for the first time coverage of the parameter space, which is intended to be probed by other searches, and either to exclude or observe the X boson in the run 2017 with the NA64 experiment.

The experiment could exploit the H4 beam-line at the CERN SPS, which can provide electrons with an energy up to $\gtrsim 150$ GeV. The detector consists of a compact, specially designed scintillator-tungsten electromagnetic (e-m) calorimeter of a high longitudinal hermeticity, additionally protected against the energy leak by high efficiency veto counters. It is also equipped with the tracker, beam defining scintillator counters, HCAL, and synchrotron

radiation detectors which provide information for a high-purity tagging of the incoming electrons.

The feasibility study of the proposed search performed in a short run in October 2016 combined with extensive simulations show that with accumulated $n_{eot} \simeq 10^{11}$ electrons on target (eot) within about 2 weeks of running at H4 the projected sensitivity for the search of the $X \to e^+e^-$ decay mode is high enough to observe X if its coupling is lying in the range $2 \times 10^{-4} \lesssim \epsilon_e < 10^{-3}$. In case of non-observation the search will exclude a significant fraction of the X parameters space.

The experiment could be performed in two phases. In phase I in 2017, the goal is to optimize the detector components, to perform the search and measure the dominant backgrounds from the punch-through photons and hadrons (and possibly muons) contaminating the electron beam. In case of non-observation the goal for phase II in 2018 would be to run the experiment in another detector configuration and at higher energy $\simeq 150$ GeV in order to reach the maximal sensitivity for the coupling strength in the region $10^{-3} < \epsilon_e < 2 \times 10^{-3}$ and fully exploit the potential of the detector after a possible upgrade, which might be necessary given the results of phase I. To reach this goal, accumulating a few 10^{10} eot at 150 GeV is mandatory. If an excess consistent with the signal hypothesis is observed, this would unambiguously indicate the presence of new physics.

References

[1] A. Krasznahorkay et al., Observation of Anomalous Internal Pair Creation in 8Be: A Possible Indication of a Light, Neutral Boson, Phys. Rev. Lett. 116, 042501 (2016).

[2] J. Feng J. L. Feng, B. Fornal, I. Galon, S. Gardner, J. Smolinsky, T. M. P. Tait, Ph. Tanedo, Phys. Rev. Lett. 117, 071803 (2016)

[3] J. L. Feng, B. Fornal, I. Galon, S. Gardner, J. Smolinsky, T. M. P. Tait, Ph. Tanedo, Phys. Rev. D 95, 035017 (2017)

[4] S. N. Gninenko, "Search for MeV dark photons in a light-shining-through-walls experiment at CERN", Phys. Rev. D89 (2014) 075008; arXiv:1308.6521 [hep-ph].

[5] A. Andreas et al., "Proposal for an Experiment to Search for Light Dark Matter at the SPS", CERN-SPSC-2013-034; SPSC-P-348 (2013), arXiv:1312.3309 [hep-ex].

[6] D. Banerjee et al. [NA64 collaboration], "Search for invisible decays of sub-GeV dark photons in missing-energy events at the CERN SPS", Phys. Rev. Lett. 118, 011802 (2017).

[7] http://cern.ch/sba

[8] S.N. Gninenko, N.V. Krasnikov, M.M. Kirsanov, D.V. Kirpichnikov, Phys. Rev. D 94, 095025 (2016)

[9] J. L. Feng, Ann. Rev. Astron. Astrophys. **48**, 495 (2010) [arXiv:1003.0904 [astro-ph.CO]].

[10] L. B. Okun, Sov. Phys. JETP **56**, 502 (1982) [Zh. Eksp. Teor. Fiz. **83**, 892 (1982)].

[11] B. Holdom, Phys. Lett. B **166**, 196 (1986).

[12] S. N. Gninenko and J. Redondo, Phys. Lett. B **664**, 180 (2008) [arXiv:0804.3736 [hep-ex]].

[13] J. Jaeckel and A. Ringwald, Ann. Rev. Nucl. Part. Sci. **60**, 405 (2010) [arXiv:1002.0329 [hep-ph]].

[14] J. L. Hewett, H. Weerts, R. Brock, J. N. Butler, B. C. K. Casey, J. Collar, A. de Gouvea and R. Essig *et al.*, arXiv:1205.2671 [hep-ex].

[15] R. Essig, J. A. Jaros, W. Wester, P. H. Adrian, S. Andreas, T. Averett, O. Baker and B. Batell *et al.*, arXiv:1311.0029 [hep-ph].

[16] M. Pospelov, A. Ritz and M. B. Voloshin, Phys. Lett. B **662**, 53 (2008) [arXiv:0711.4866 [hep-ph]].

[17] E. J. Chun, J. -C. Park and S. Scopel, JHEP **1102**, 100 (2011) [arXiv:1011.3300 [hep-ph]].

[18] Y. Mambrini, JCAP **1107**, 009 (2011) [arXiv:1104.4799 [hep-ph]].

[19] S. Andreas, M. D. Goodsell and A. Ringwald, Phys. Rev. D **87**, 025007 (2013) [arXiv:1109.2869 [hep-ph]].

[20] D. Hooper, N. Weiner and W. Xue, Phys. Rev. D **86**, 056009 (2012) [arXiv:1206.2929 [hep-ph]].

[21] H. Davoudiasl and I. M. Lewis, arXiv:1309.6640 [hep-ph].

[22] H. Davoudiasl, H. -S. Lee, I. Lewis and W. J. Marciano, Phys. Rev. D **88**, 015022 (2013) [arXiv:1304.4935 [hep-ph]].

[23] J. Jaeckel, Frascati Phys. Ser. **56**, 172 (2012) [arXiv:1303.1821 [hep-ph]].

[24] B. Batell, M. Pospelov and A. Ritz, Phys. Rev. D **80**, 095024 (2009) [arXiv:0906.5614 [hep-ph]].

[25] M. Reece and L. -T. Wang, JHEP **0907**, 051 (2009) [arXiv:0904.1743 [hep-ph]].

[26] M. Williams, C. P. Burgess, A. Maharana and F. Quevedo, JHEP **1108**, 106 (2011) [arXiv:1103.4556 [hep-ph]].

[27] J. D. Bjorken, R. Essig, P. Schuster and N. Toro, Phys. Rev. D **80**, 075018 (2009) [arXiv:0906.0580 [hep-ph]].

[28] S. Andreas, C. Niebuhr and A. Ringwald, Phys. Rev. D **86**, 095019 (2012) [arXiv:1209.6083 [hep-ph]].

[29] A. Konaka, K. Imai, H. Kobayashi, A. Masaike, K. Miyake, T. Nakamura, N. Nagamine and N. Sasao *et al.*, Phys. Rev. Lett. **57**, 659 (1986).

[30] E. M. Riordan, M. W. Krasny, K. Lang, P. De Barbaro, A. Bodek, S. Dasu, N. Varelas and X. Wang *et al.*, Phys. Rev. Lett. **59**, 755 (1987).

[31] J. D. Bjorken, S. Ecklund, W. R. Nelson, A. Abashian, C. Church, B. Lu, L. W. Mo and T. A. Nunamaker *et al.*, Phys. Rev. D **38**, 3375 (1988).

[32] M. Davier and H. Nguyen Ngoc, Phys. Lett. B **229**, 150 (1989).

[33] A. Bross, M. Crisler, S. H. Pordes, J. Volk, S. Errede and J. Wrbanek, Phys. Rev. Lett. **67**, 2942 (1991).

[34] J. Blumlein and J. Brunner, Phys. Lett. B **701**, 155 (2011) [arXiv:1104.2747 [hep-ex]].

[35] H. Merkel *et al.* [A1 Collaboration], Phys. Rev. Lett. **106**, 251802 (2011) [arXiv:1101.4091 [nucl-ex]].

[36] S. Abrahamyan *et al.* [APEX Collaboration], Phys. Rev. Lett. **107**, 191804 (2011) [arXiv:1108.2750 [hep-ex], arXiv:1108.2750 [hep-ex]].

[37] J. Bluemlein and J. Brunner, arXiv:1311.3870 [hep-ph].

[38] T. Beranek and M. Vanderhaeghen, arXiv:1311.5104 [hep-ph].

[39] F. Archilli, D. Babusci, D. Badoni, I. Balwierz, G. Bencivenni, C. Bini, C. Bloise and V. Bocci *et al.*, Phys. Lett. B **706**, 251 (2012) [arXiv:1110.0411 [hep-ex]].

[40] H. -B. Li and T. Luo, Phys. Lett. B **686**, 249 (2010) [arXiv:0911.2067 [hep-ph]].

[41] B. Aubert *et al.* [BaBar Collaboration], Phys. Rev. Lett. **103**, 081803 (2009) [arXiv:0905.4539 [hep-ex]].

[42] S. N. Gninenko, Phys. Rev. D **87**, 035030 (2013) [arXiv:1301.7555 [hep-ph]].

[43] R. Meijer Drees *et al.* [SINDRUM I Collaboration], Phys. Rev. Lett. **68**, 3845 (1992).

[44] P. Adlarson *et al.* [WASA-at-COSY Collaboration], Phys. Lett. B **726**, 187 (2013) [arXiv:1304.0671 [hep-ex]].

[45] G. Agakishiev *et al.* [HADES Collaboration], arXiv:1311.0216 [hep-ex].

[46] S. N. Gninenko, Phys. Rev. D **85**, 055027 (2012) [arXiv:1112.5438 [hep-ph]].

[47] S. N. Gninenko and N. V. Krasnikov, Phys. Lett. B **427**, 307 (1998) [hep-ph/9802375].

[48] J. Altegoer *et al.* [NOMAD Collaboration], Phys. Lett. B **428**, 197 (1998) [hep-ex/9804003].

[49] P. Astier *et al.* [NOMAD Collaboration], Phys. Lett. B **479**, 371 (2000).

[50] S. N. Gninenko, Nucl. Phys. Proc. Suppl. **87**, 105 (2000).

[51] S. Weinberg, Phys. Rev. D **26**, 287 (1982). P. Fayet, Nucl. Phys. B **187**, 184 (1981).

[52] S. N. Gninenko and N. V. Krasnikov, Phys. Lett. B **513**, 119 (2001) [hep-ph/0102222].

[53] M. Masip, P. Masjuan and D. Meloni, JHEP **1301**, 106 (2013) [arXiv:1210.1519 [hep-ph]].

[54] A. Radionov, Phys. Rev. D **88**, 015016 (2013) [arXiv:1303.4587 [hep-ph]].

[55] S. Andreas, "Light Weakly Interacting Particles: Constraints and Connection to Dark Matter," 2013, 200 pp, DESY-THESIS-2013-024.

[56] See, for example, http://sba.web.cern.ch/sba/, and, also http://nahandbook.web.cern.ch/.

[57] S. N. Gninenko, arXiv:1308.6521 [hep-ph].

[58] Yu. Musienko, private communication.

[59] S. Agostinelli *et al.* [GEANT4 Collaboration], Nucl. Instrum. Meth. A **506**, 250 (2003). J. Allison, K. Amako, J. Apostolakis, H. Araujo, P. A. Dubois, M. Asai, G. Barrand and R. Capra *et al.*, IEEE Trans. Nucl. Sci. **53**, 270 (2006).

[60] S. N. Gninenko, Nucl. Instrum. Meth. A **409**, 583 (1998).

[61] D. Autiero, M. Baldo-Ceolin, F. Bobisut, L. Camilleri, P. W. Cattaneo, V. Cavasinni, D. Collazuol and G. Conforto *et al.*, Nucl. Instrum. Meth. A **411**, 285 (1998).

[62] W. Flauger and F. Monnig, Nucl. Phys. B **109**, 347 (1976).

[63] J. Engler, B. Gibbard, W. Isenbeck, F. Monnig, J. Moritz, K. Pack, K. H. Schmidt and D. Wegener *et al.*, Nucl. Phys. B **84**, 70 (1975).

[64] S. N. Gninenko, Phys. Lett. B **713**, 244 (2012) [arXiv:1204.3583 [hep-ph]].

[65] S. I. Bityukov and N. V. Krasnikov, Mod. Phys. Lett. A **13**, 3235 (1998).

[66] S. I. Bityukov and N. V. Krasnikov, Nucl. Instrum. Meth. A **534**, 152 (2004).

[67] M. Endo, K. Hamaguchi and G. Mishima, Phys. Rev. D **86**, 095029 (2012) [arXiv:1209.2558 [hep-ph]].

[68] M. Pospelov, Phys. Rev. D **80**, 095002 (2009) [arXiv:0811.1030 [hep-ph]].

[69] R. Essig, J. Mardon, M. Papucci, T. Volansky and Y. -M. Zhong, arXiv:1309.5084 [hep-ph].

[70] P. Adzic *et al.* [CMS Collaboration], JINST **5**, P03010 (2010) [arXiv:0912.4300 [physics.ins-det]].

[71] J. S. Dworkin, P. T. Cox, E. C. Dukes, O. E. Overseth, R. Handler, R. Grobel, A. Jaske and B. Lundberg *et al.*, Nucl. Instrum. Meth. A **247**, 412 (1986).

[72] N. V. Krasnikov *et al.*, work in progress.

[73] E. Izaguirre, G. Krnjaic, P. Schuster and N. Toro, arXiv:1307.6554 [hep-ph].

[74] T. Beranek and M. Vanderhaeghen, Phys. Rev. D **87**, 015024 (2013) [arXiv:1209.4561 [hep-ph]].

[75] P. deNiverville, M. Pospelov and A. Ritz, Phys. Rev. D **84**, 075020 (2011) [arXiv:1107.4580 [hep-ph]].